

RESISTIVITY MEASUREMENTS IN THE TOROIDAL DISCHARGE IN AN OCTUPOLE

J. F. Etzweiler & J. C. Sprott

(talk given at the Nov. 1975 meeting of the Plasma Physics Division of APS,
St. Petersburg, Florida)

PLP 674

Plasma Studies

University of Wisconsin

These PLP Reports are informal and preliminary and as such may contain errors not yet eliminated. They are for private circulation only and are not to be further transmitted without consent of the authors and major professor.

In this paper, we report the results of extending plasma resistivity measurements into a higher plasma density regime. Six years ago Lencioni^{1,2} observed the scaling in the small octupole:

$$\eta_L = 2.5 \times 10^7 \sqrt{T_e} / n_e \quad \Omega\text{-m}$$

where $5 \times 10^7 < n_e < 2 \times 10^9 / \text{cm}^3$ and $T_e \stackrel{N}{\approx} 3 \text{ eV}$. We observe the same inverse dependence on density with the same numerical factor for $10^{10} < n_e < 2 \times 10^{12} / \text{cm}^3$. At the higher densities Spitzer resistivity η_{sp} for $z = 1$ starts to dominate.

In addition, we have observed classical, that is, collisional resistivity for high filling pressures where electron collisions with neutral hydrogen become important.

Description of Experiment

The first figure shows the lines of constant poloidal magnetic flux in the small Wisconsin supported toroidal octupole.

A toroidal magnetic field is provided by a 24 turn external winding. Resistivity measurements are made near the center of the machine, in the region where the octupole field is very small. Here the decay of the poloidal magnetic flux generates an electric field parallel to the toroidal magnetic field. The plasma toroidal current density j_T is measured near its spatial peak using a paddle probe^{1,2,3,4,5,6} with surface area 1.0 mm^2 . Since the plasma current is small compared with the current in the hoops, the toroidal electric field E_T is approximately the vacuum field.

$$E_T = .95 V \sin (.54 (t-2.4)) \quad \text{V/m}$$

where V is the voltage in kV on the octupole capacitor bank and t is the time from the octupole field trigger. The measured parallel resistivity is then given by

$$\eta_m = E_T / j_T.$$

The operating parameters for this ohmic heating experiment are shown in Figure 2. The octupole field B_p pulse is a half sine wave lasting 5 ms. The toroidal field B_T pulse is a damped half sine wave lasting 2 ms with its peak at .8 ms. The relative delay is 3.5 ms, chosen experimentally to maximize toroidal current density. The plasma is prepared with electron cyclotron resonance heating (ECRH) microwaves, which are turned off when B_T is turned on.

The range of fields available on axis are $.7 < E_T < 4$ V/m and $0 < B_T < 1.8$ kG. Most of the data presented here was obtained for peak $B_T = 1.2$ kG on axis. Plasma parameters fill the range $10^{10} < n_e < 2 \times 10^{12}/\text{cm}^3$ and $3 < T_e < 30$ eV as measured with Langmuir probes using simple probe theory assuming a Maxwellian electron velocity distribution function $f_e(v)$. Since operating conditions approach the electron runaway regime, $f_e(v)$ may actually have a double peak and/or an enhanced tail. Therefore, the interpretation of probe measurements of T_e is questionable. Methods used were swept probe,⁷ admittance probe⁸ and floating triple probe,⁹ all giving T_e within the same range.

Experimental Results

Two typical data runs are displayed in Figure 3. Resistivity η is plotted against real H_2 filling pressure. The experimentally measured η_m is shown as x's. Triangles represent η_{Sp} calculated from the measured T_e assuming $z = 1$. Squares represent resistivity due to electron collisions with neutral hydrogen calculated from the measured n_e assuming neutral density is given by subtracting n_e from the filling density:

$$\eta_n = .3 \times 10^{-5} \left(\frac{2n_{H2}}{n_e} - 1 \right) \quad \Omega\text{-m},$$

where $\overline{\sigma v}$ is taken from a graph in Rose and Clark.¹⁰ Circles represent the total collisional or classical resistivity

$$\eta_{col} = \eta_{Sp} + \eta_n.$$

For high filling pressures ($p \gtrsim 1 \times 10^{-4}$ Torr) the measured resistivity matches classical scaling. For the upper graph, where the fractional ionization n_e/n_H is relatively high, η_{Sp} dominates η_{col} up to 2×10^{-4} Torr. For the lower graph where n_e/n_H is less, η_n dominates for $p \geq 1 \times 10^{-4}$ Torr.

For the lower filling pressures ($p \lesssim 1 \times 10^{-4}$ Torr) η_m becomes anomalous, that is, non-classical. Figure 4 shows more clearly the transition from classical scaling at high pressure to anomalous scaling at low pressure for the same data as in Figure 3.

Analysis

The issue of interest becomes the scaling of and, if possible, an explanation for the anomalous resistivity measured at low pressure. One suspects that the presence of runaway electrons might cause a current-limiting instability. Without pursuing this point further, we note that, although the toroidal electric field E_T is less than the critical field E_{crit} for average electrons to run away,¹¹ the ratio η_m/η_{col} tends to increase with increasing E_T/E_{crit} . This trend is shown in Figure 5. The suggestion is that as a higher fraction of electrons becomes capable of running away, the resistivity is increasingly affected.

Attempts are made to determine the scaling of resistivity with electron density and temperature. Despite the difficulty of varying only one parameter without changing any of the others, some preliminary data was obtained and is displayed in logarithmic plots in Figures 6 and 7. Figure 6 shows the inverse proportionality between resistivity and plasma density, while the variation of T_e in Figure 7 seems to have very little effect on resistivity.

The apparent inverse density dependence calls to mind the resistivity measured by Lencioni^{1,2} and referred to in the first paragraph of this paper.

When Lencioni's resistivity is added to the calculated collisional resistivity and compared with the data in Figures 3 and 4, the plot in Figure 8 is obtained. This graph shows the low pressure anomalous data only. The square data points correspond to the lower graphs in Figures 3 and 4 while the circles correspond to the upper graphs. Adding collisional and Lencioni resistivity seems to give the right form for at least some of the data, but the magnitude seems to be low by a factor of two. Experimental errors may well be the reason. The departure of the very low pressure data from a horizontal line is due to variations in temperature T_e which is probably the most inaccurately measured of all the experimental quantities. On the other hand, our observed lack of resistivity dependence on T_e may be valid and thus in disagreement with both Lencioni's observations and with collisional theory. Thus, the scaling of anomalous resistivity with all parameters remains incompletely known and unexplained where it is known.

Conclusion

The most significant result of these measurements so far is the observation of anomalous resistivity inversely proportional to electron density over five orders of magnitude. The combined data from Lencioni's and our work is shown in Figure 9. Our data is plotted regardless of measured T_e whose variation has an incompletely documented effect or lack of effect on resistivity. For large enough neutral densities, resistivity is fully explained by collisions with neutral particles, and for large enough electron densities (approaching $10^{13}/\text{cm}^3$) Spitzer resistivity becomes large enough to dominate in the observed range of T_e .

References

1. D. E. Lencioni, Phys. Fluids 14, 566 (1971); same as PLP 329 (Feb., 1970).
2. D. E. Lencioni, Ph.D. Thesis, Univ. of Wis. (1969); same as PLP 276 (May, 1969).
3. E. I. Urazakov and V. L. Granovskii, Sov. Phys. JETP 14, 981 (1962).
4. J. A. Schmidt, PLP 123 (May, 1967).
5. E. A. Bering, M. C. Kelley, F. S. Mozer, and U. V. Fahleson, Planet. Space Sci. 21, 1983 (1973).
6. J. F. Etzweiler, PLP 619 (April, 1975).
7. F. F. Chen, Plasma Diagnostic Techniques, ed: R. H. Huddlestone and S. L. Leonard (Academic Press, Inc., N.Y., 1965), Chap. 4.
8. J. C. Sprott, PLP 74 (July, 1966), PLP 176 (Jan., 1968), and PLP 185 (March, 1968).
9. To be discussed in a future PLP.
10. D. J. Rose and M. Clark, Jr., Plasmas and Controlled Fusion (M.I.T. Press, Cambridge, Mass., 1961); p. 30.
11. H. Dreicer, Phys. Rev. 115, 238 (1959).

WISCONSIN
SUPPORTED
TOROIDAL
OCTUPOLE

surfaces
of constant
poloidal magnetic
flux

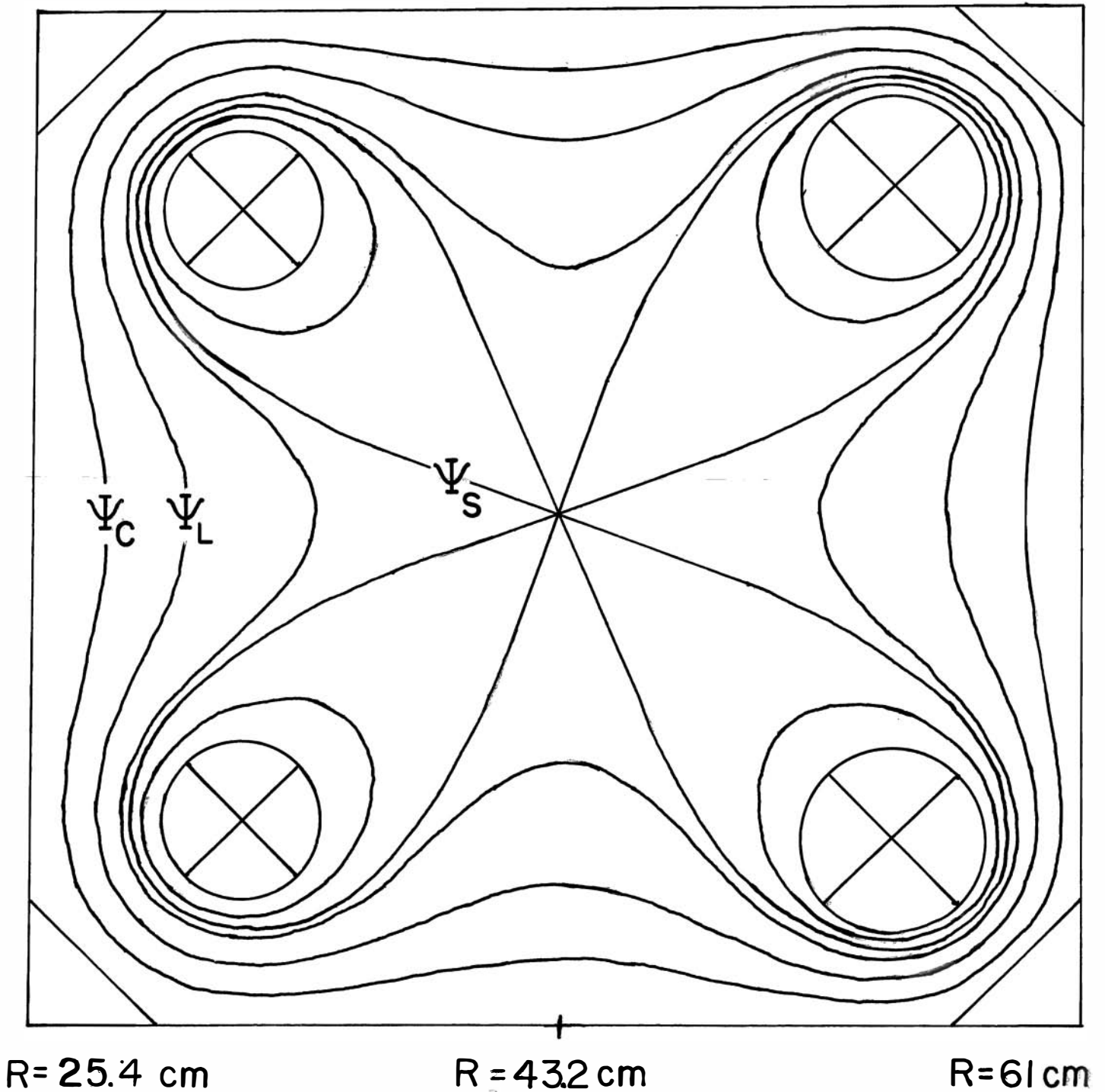
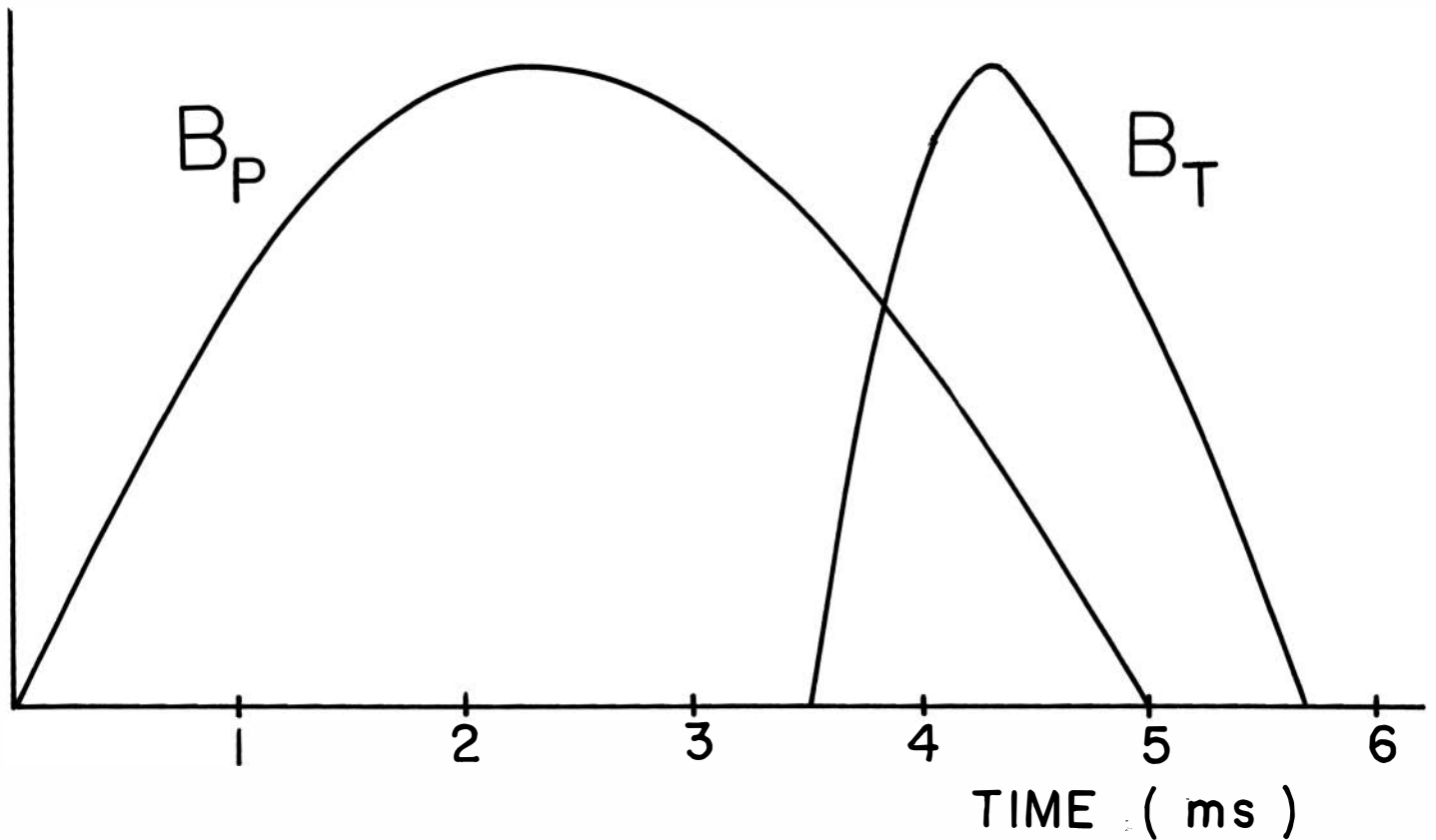


Figure 1.



OHMIC HEATING EXPERIMENT PARAMETERS

FIELDS on axis

$$E_T = .8 - 5.0 \text{ V/m}$$

$$\text{max. } B_T = 1.8 \text{ kG}$$

PLASMA

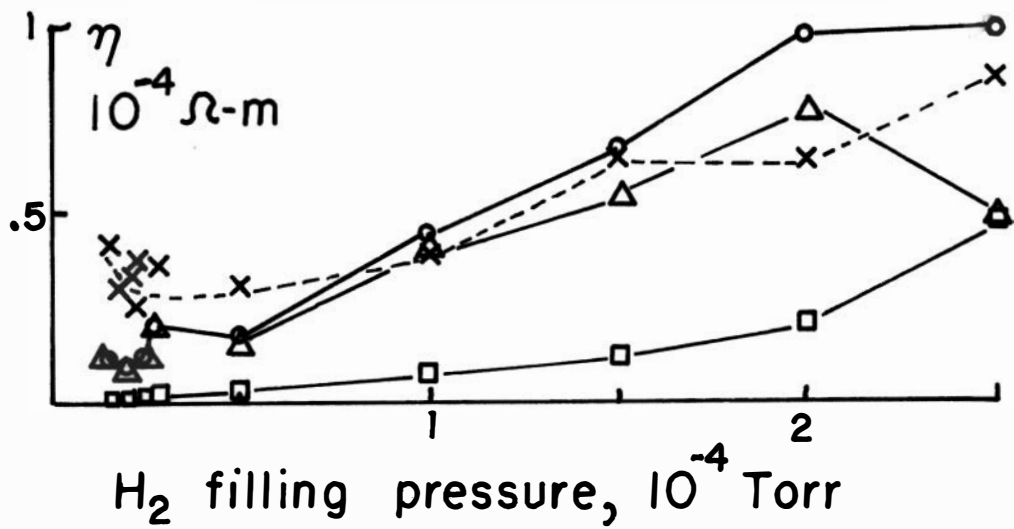
$$n_e = 10^{10} - 10^{12} / \text{cm}^3$$

$$T_e = 2 - 30 \text{ eV}$$

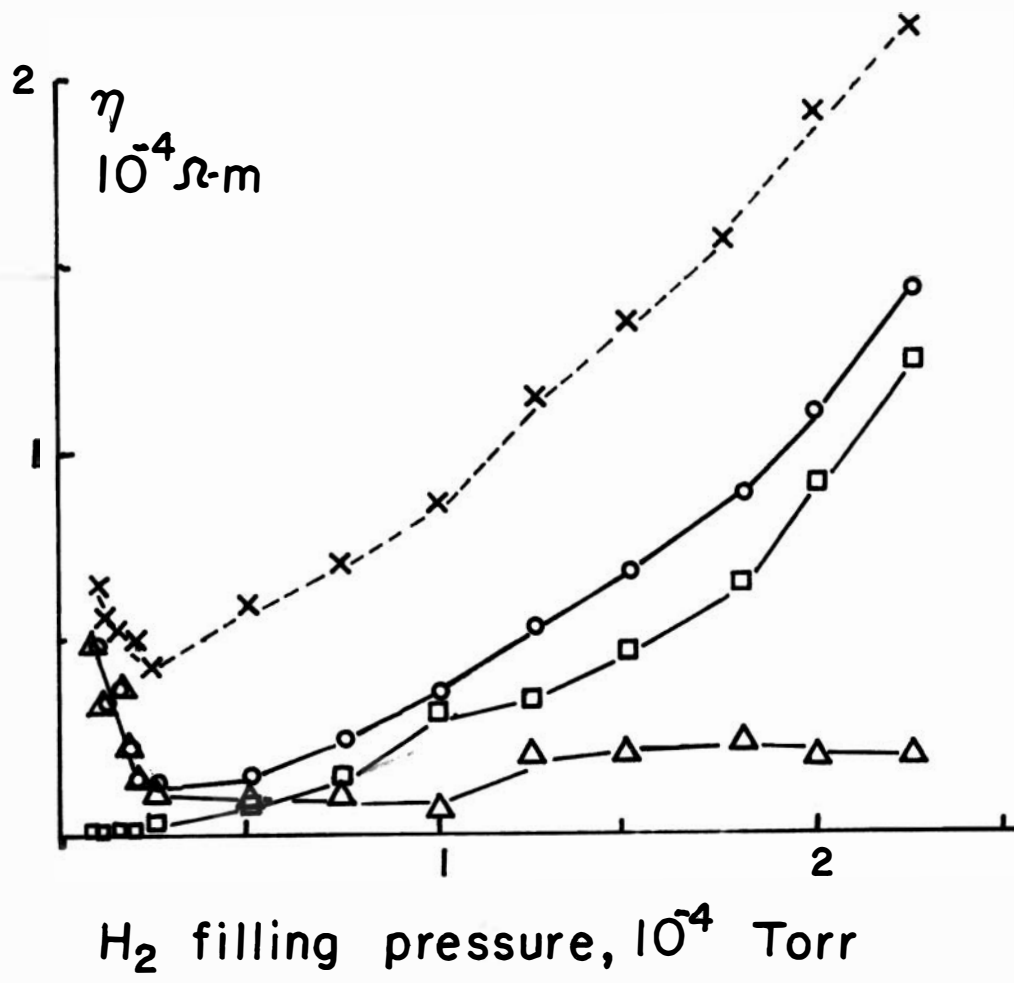
ECRH pre ionization

Figure 2.

Theory and Experiment: η vs. p



high n_e/n_H
for large p



low n_e/n_H
for large p

- x - experiment
- o - total collisional
- - neutrals only
- △ - Spitzer only

Figure 3.

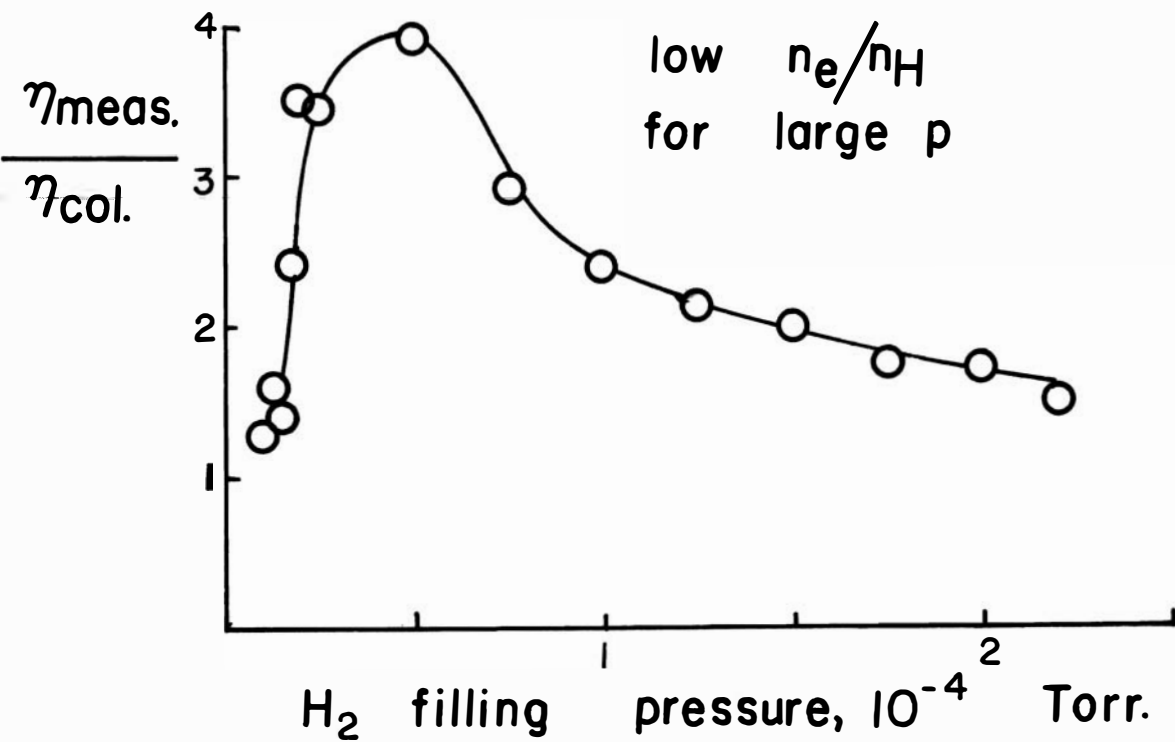
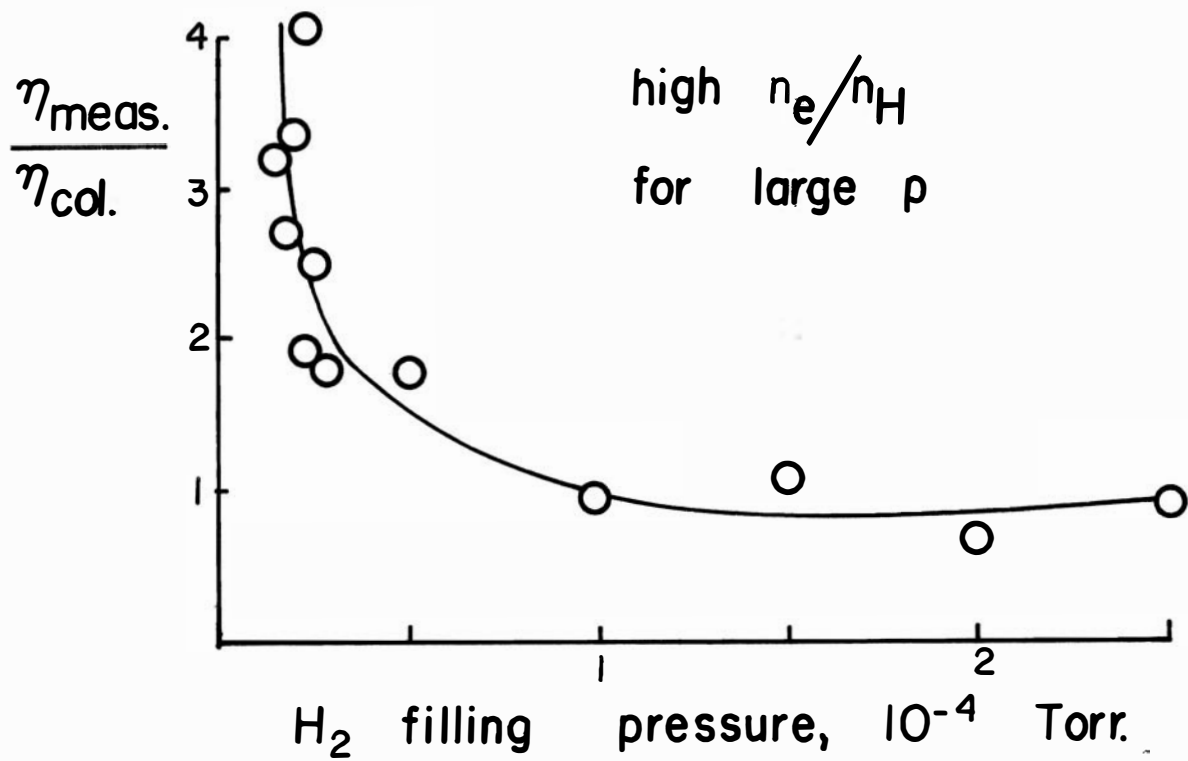


Figure 4.

$$\eta_{\text{meas}} / \eta_{\text{col}} \propto (E_T / E_{\text{crit}})^X, \quad 1 \lesssim X \lesssim 2$$

$$\text{low } p \Leftrightarrow \eta_{\text{col}} \approx \eta_{\text{sp}}$$

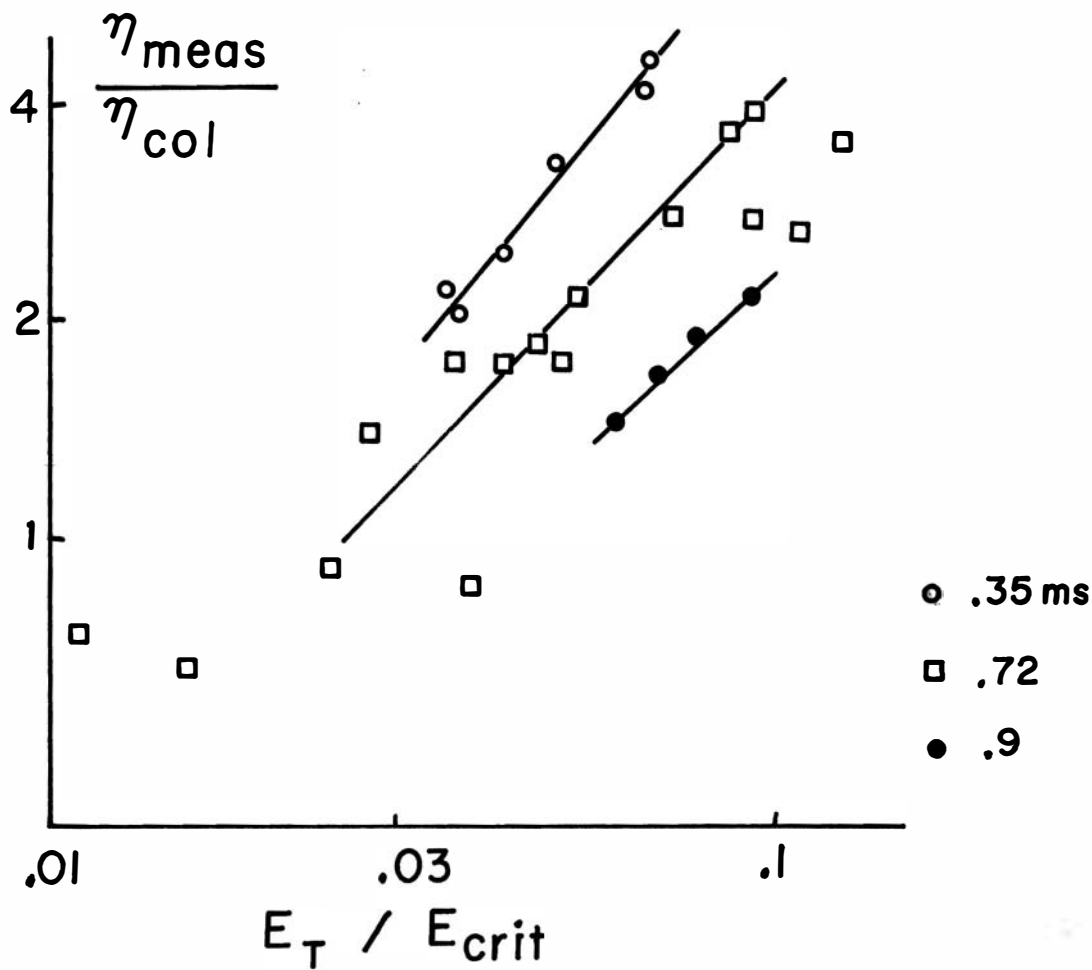


Figure 5.

$$\eta_{\text{meas}} \sim 1/n_e^x, \quad .6 \lesssim x \lesssim 1$$

low p

$$T_e = 6.2 \pm 1.2 \text{ eV}$$

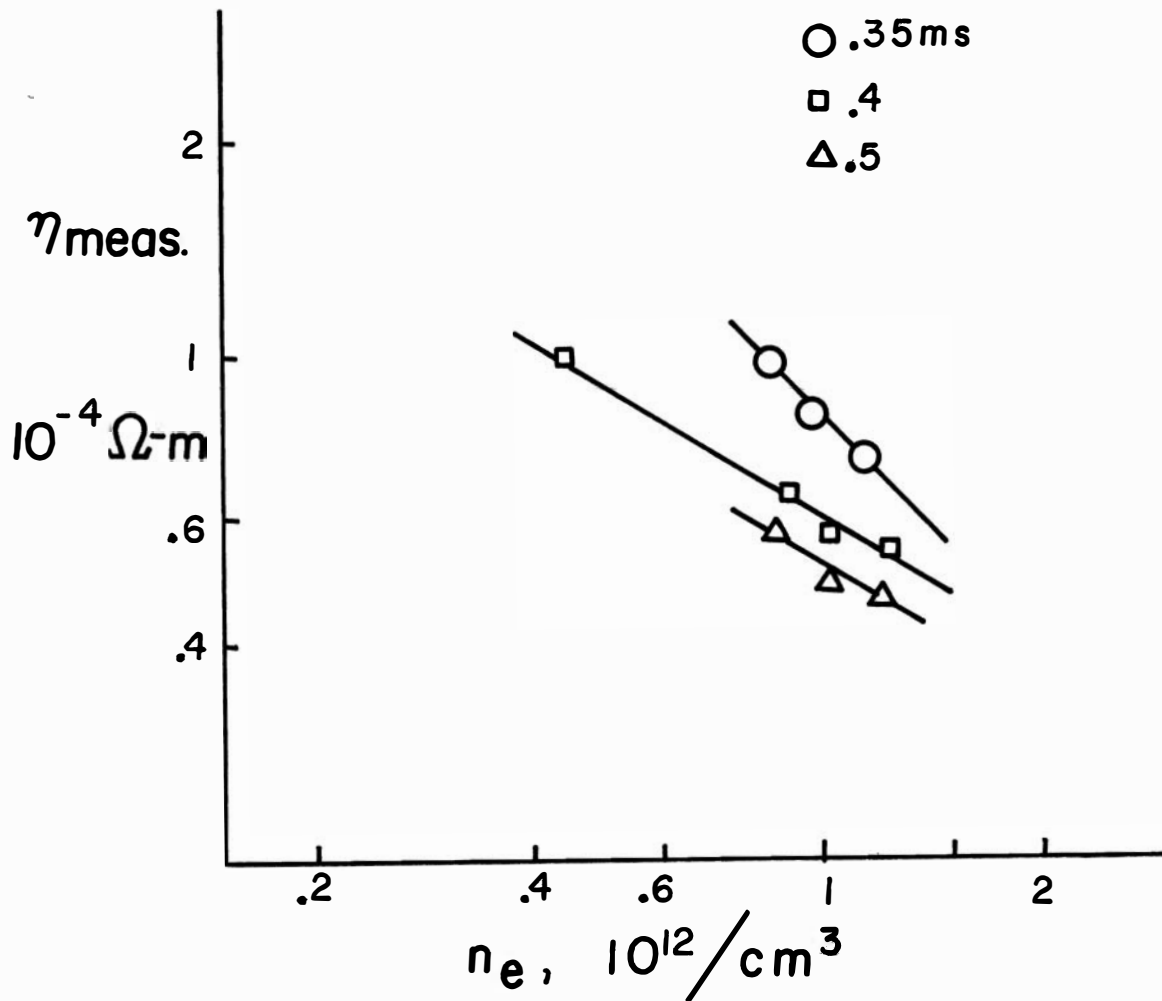


Figure 6.

$$\eta_{\text{meas.}} \sim (1/T_e)^x, \quad 0 \lesssim x \lesssim .2$$

low p

$$n_e = 1.07 \pm .07 \times 10^{12} / \text{cm}^3$$

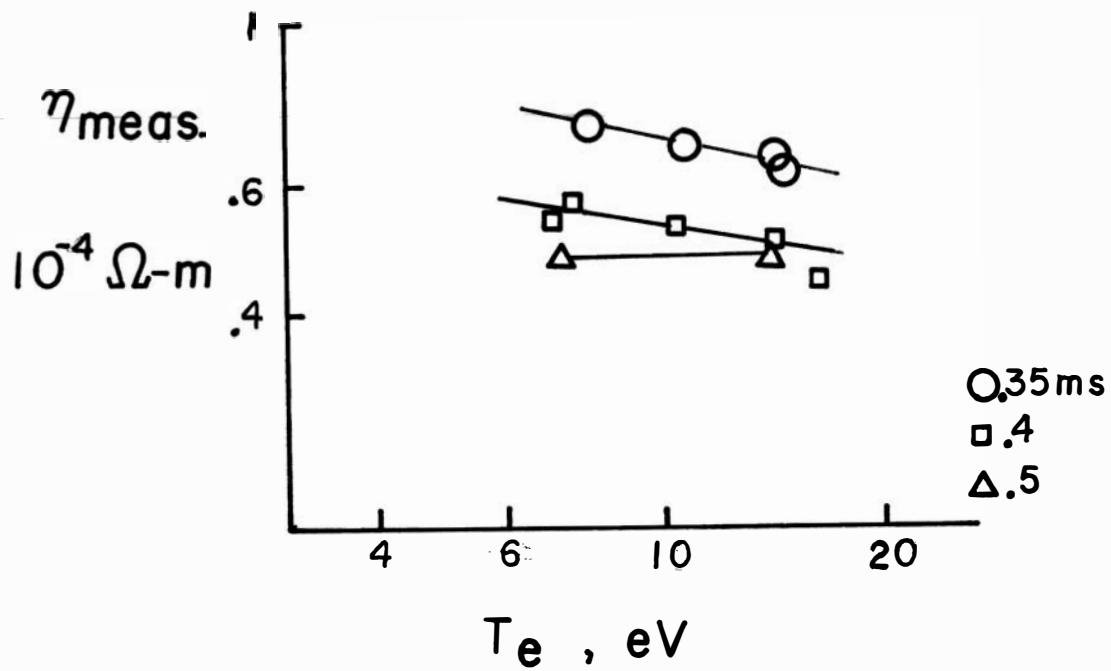


Figure 7.

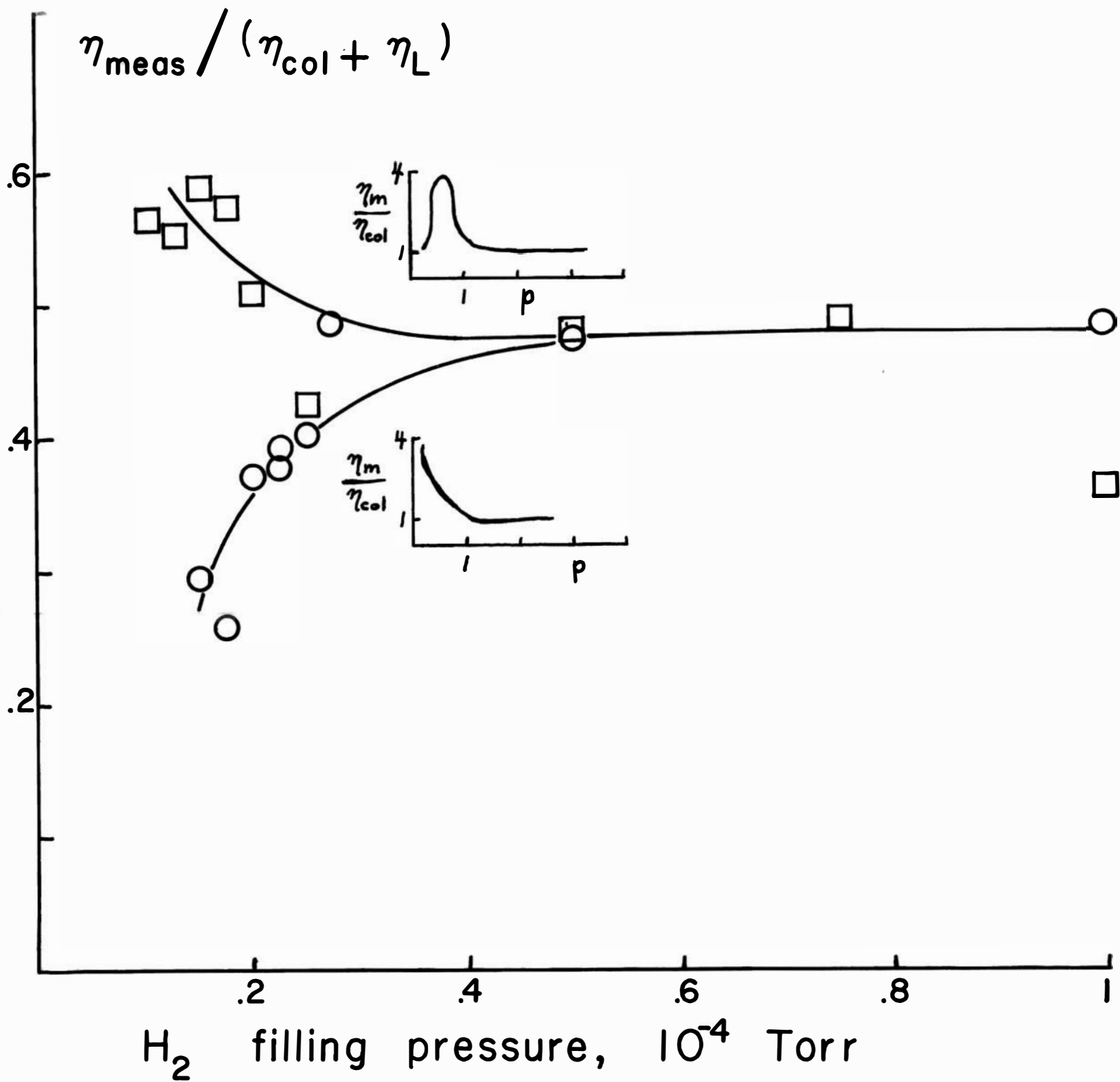


Figure 8.

Lencioni (1969)

plasma gun

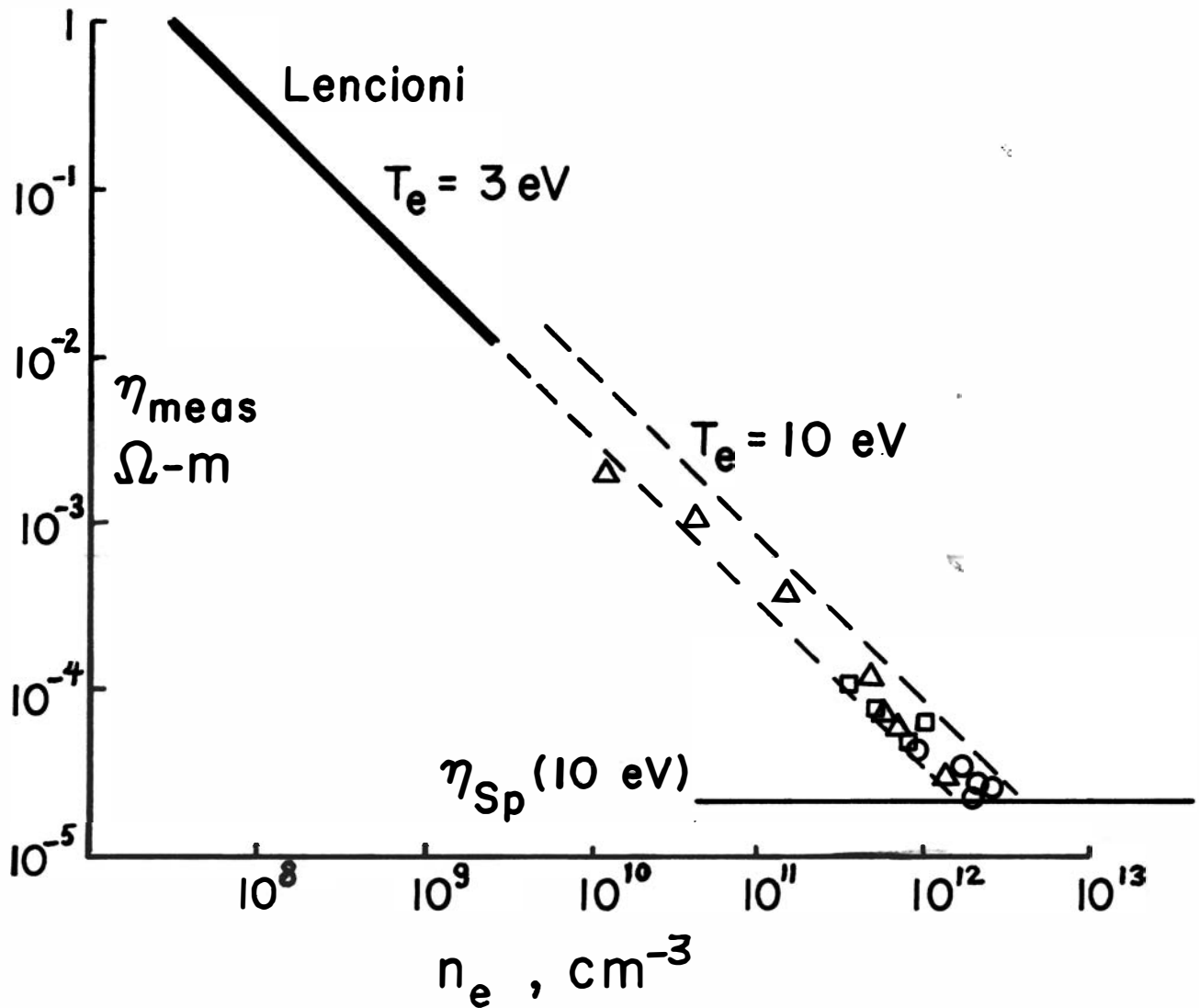
$$E_T/E_{crit} = 70-1000$$

$$\eta_{meas} = 2.5 \times 10^7 \sqrt{T_e} / n_e$$

Etzweiler & Sprott (1975)

μ wave plasma

$$E_T/E_{crit} = .01 - .1$$



Δ B_p varied, admittance probe

\circ p varied, swept probe

\square " " , floating triple probe

Figure 9.